



Enhancement of the performance of Photovoltaic/Trombe wall system using the porous medium: Experimental and theoretical study



Omer K. Ahmed ^{a,*}, Khalaf I. Hamada ^b, Abdulrazzaq M. Salih ^b

^a Technical College/Kirkuk, Northern Technical University, Iraq

^b College of Engineering, Tikrit University, Iraq

ARTICLE INFO

Article history:

Received 3 September 2018

Received in revised form

27 November 2018

Accepted 1 January 2019

Available online 4 January 2019

Keywords:

PV/Trombe wall

Performance

Porous

Medium

Effect

ABSTRACT

The hybrid Photovoltaic/Thermal systems are suffering from the low electrical performance as a result of elevated its temperature. Present work attempts to enhance the performance of a hybrid Photovoltaic/Trombe wall (PV/TW) system through employing a porous medium. In this article, the effect of porous medium, DC fan and glass cover on the performance of a PV/TW was accomplished by the design and implementation of an experimental system to achieve this target. The mathematical method to predict the performance of a PV/TW system was also offered based on a simplified concept of an energy balance. The results of the theoretical study agreed well with the practical results in terms of the estimated temperature of the solar cell.

The results revealed that incorporating the porous medium and DC fan offered favorable features of the system performance, while the glass cover has a conflict effect. It was confirmed that using porous medium and DC fan reduces the temperature of PV cell and increases the room temperature. Whereas, the presence of the glass cover in front of the system leads to elevate the temperatures of the room and solar cell. The presence of porous medium with DC fan increases the values of thermal and electrical efficiencies about 13% and 4%, respectively. Furthermore, the combined effect of porous medium with DC fan and glass cover increases the values of thermal and electrical efficiencies about 20% and 0.5%, respectively. It is recommended to integrate the PV/TW system with DC fan and porous medium for further conversion of solar radiation and improve building comfort conditions.

© 2019 Elsevier Ltd. All rights reserved.

1. Introduction

The world today is facing the energy crisis, as it has become one of the most important problems due to the large and continuous increase in energy consumption that depletes conventional energy sources. In addition, there is a limited reserve of conventional energy resources, as well as a significant rise in fuel prices and environmental problems [1]. Research and studies have begun focusing on renewable energy, especially solar energy, to address conventional energy problems and replace it with a clean and environmentally friendly option [2].

The Trombe wall is one of the passive solar systems that take advantage of the available solar energy in nature and converts it into heat without any electrical or mechanical assistance. A Trombe wall is always fixed on the southern façade of buildings in the

northern hemisphere to increase solar energy throughout the year. The principles of the Trombe wall are described as shown in Fig. 1. It consists of a wall of concrete for heat storage and the wall is dyed with a black color to increase absorption of solar radiation. There are layers of glass at 5–10 cm distance from the concrete wall to increase the intensity of solar radiation [3].

In the past decades, modern technologies that use solar cells to generate electricity have been introduced. A photovoltaic (PV) cell can be integrated with buildings in diverse ways (rooftops, façades, PV/Trombe wall (PV/TW),...etc.). The PV cell in such hybrid system not only produces the electricity but also helps in heating, day lighting, and reduces cooling/heating loads, as well adds the aesthetic of the building [4]. Generally, these hybrid systems can be classified into PV/Trombe wall, building-integrated photovoltaic (BIPV) system, and PV/thermal collector. These hybrid systems are more efficient than separate solar thermal and electrical systems [5,6].

PV/TW system considers favorable architectural technology and utilizes solar energy for generating electricity as well as cooling and

* Corresponding author.

E-mail address: omerkalil@yahoo.com (O.K. Ahmed).

Nomenclatures:

G	Solar radiation (W/m^2)
E	The power output of the PV modules (W)
T_c	Temperatures of the solar cell ($^{\circ}\text{C}$)
T_f	Temperatures of air flow ($^{\circ}\text{C}$)
T_a	Ambient temperature ($^{\circ}\text{C}$)
T_{wall}	The temperature of the outside surface wall ($^{\circ}\text{C}$)
T_{out}	Air temperatures of outlet duct ($^{\circ}\text{C}$)
T_{in}	Air temperatures of inlet duct ($^{\circ}\text{C}$)
T_p	The temperature of plate aluminum ($^{\circ}\text{C}$)
T_{pm}	Temperature of porous medium ($^{\circ}\text{C}$)
\dot{m}_f	The mass flow rate of air (kg/s)
c_{pf}	Specific heat of air (J/kg.K)
$h_{\text{c,c-a}}$	Heat transfer coefficient for convection on the outside surface of the solar cell ($\text{W/m}^2.\text{K}$)
$h_{\text{r,c-a}}$	Heat transfer coefficients for radiation on the outside of the solar cell ($\text{W/m}^2.\text{K}$)
$h_{\text{c,p-f}}$	Convection heat transfer coefficient from the back surface of aluminum plate to air flow ($\text{W/m}^2.\text{K}$)
$h_{\text{r,p-f}}$	Radiant heat transfer coefficients coefficient from the back surface of aluminum plate to air flow ($\text{W/m}^2.\text{K}$)
$h_{\text{r,pm-f}}$	Radiation coefficient of heat transfer from porous medium to the air in the duct ($\text{W/m}^2.\text{K}$)
$h_{\text{c,pm-f}}$	Convection coefficient of heat transfer from porous medium to the air in the duct ($\text{W/m}^2.\text{K}$)
$h_{\text{c,wall-f}}$	Convection coefficient of heat transfer from wall to air in the duct ($\text{W/m}^2.\text{K}$)
V	Wind speed (m/s)
V_f	Air velocity in the air channel (m/s)
W	Width of the PV/Trombe wall (m)
X	Height of the PV/Trombe wall (m)
D	The depth of the air duct (m)
A_c	Area of PV/Trombe wall (m^2)
A_m	Specific wetted area (m^2)
d_{pm}	The diameter of the glass spheres (m)
D_{hd}	The equivalent diameter of the porous medium (m)
U_T	Overall coefficient of heat transfer between solar cell to ambient ($\text{W/m}^2.\text{K}$)

U_{bottom}	Overall coefficient of heat transfer between plate aluminum to solar cell ($\text{W/m}^2.\text{K}$)
I	Electric current (A)
V_o	The voltage of the solar cell (V)

Greek Symbols

α_c	absorption factor of the solar cell
ε_1	Emissivity on the front side of the solar cell
ε_2	Emissivity on the back side of the aluminum plate
ε_c	Emissivity of the outside of the PV glass panel
ε_a	Emissivity of an ambient environment
ε_p	Emissivity of the inside of the plate aluminum
ε_{pm}	Emissivity of the porous medium
$\eta_{\text{ele.s}}$	Electrical efficiency under standard conditions (%)
μ_f	dynamic viscosity of air (Kg/m.s)
ρ_f	Air density (kg/m^3)
λ_f	Thermal conductivity of air (W/m.K)
λ_{pm}	Thermal conductivity of porous medium (W/m.K)
β_{pm}	Constant depended on shape porous medium
η_{th}	Thermal efficiency (%)
η_{ele}	Electrical efficiency (%)
Φ	Porosity
β_c	Packing factor
α_p	Absorptivity's of plate
τ_g	Transmittance factor of the front cover glass of solar cell
\forall_f	A volume of fluid (m^3)
\forall_t	Total volume (m^3)

Subscripts Abbreviations

C	Solar cell
c	Convective
f	Air
g	Glass
p	Plate aluminum
pm	Porous medium
r	Radiant
si	Silicon
t	Tube
T	Total

heating in different climate areas. The structure of the PV/TW system is shown in Fig. 2. The PV panel is fixed on the south side of the room, which acts as a thermal absorber. Two air slots for heating at winter and two other slots for cooling at summer. For air heating, the winter slots are opened, while the summer air holes are closed. The air from the room enters through the lower winter slots into the air duct due to the buoyancy effect. It not only produces thermal heat and electricity but also reduces the temperature of the solar cell. The air in the duct extract the heat away from the PV panel, then enters the room. While during the summer season, the behavior is vice versa [7].

Many factors affect the efficiency of the PV/TW system and these factors should be considered when designing this system in buildings. Irshad et al. [8–10] offered a simulation model of an experimental room with PV/TW system using TRNSYS software. The effect of the mass flow rate of air and three types of glass cover on the performance of the PV/TW system was studied. The results showed that the double-glazing PV/TW system loaded with argon demonstrated a significant reduction in cooling load and room temperature, while PV productivity increased. However, the validity of there simulation model was not clarified, as well as the air

velocity estimation was not well identified. Koyunbaba and Yilmaz [11] carried out a comparison of a Trombe wall with single glazing, two-fold glazing, and PV cells in Izmir. The results showed that the two-fold glass had higher insulation properties at night, while single glazing produced a high thermal gain in daytime due to higher solar radiation transmissivity. It was recommended to remodel the system for summer cooling in order to overcome warming in summer. Although, the system should be optimized before extending its applicability for various climatic and operations conditions. Also, Koyunbaba and Yilmaz [12] evaluated the performances of fan-assisted single glazing, double glazing, and PV/TW designs. The results confirmed that the use of the fan decreases thermal efficiency and increase electrical efficiency. Also, it has been found that the insulating properties of double glass are much better than a single glass. It works to reduce heat loss to the surrounding at night and this is important for heating in winter. Also, it was noted that for winter heating is redundant to use of fan in these systems. However, it was not clear about the influence of the fan energy consumption and air velocity.

Jie et al. [13] introduced a novel system for PV/TW through connecting to a DC fan and compared the performance of the

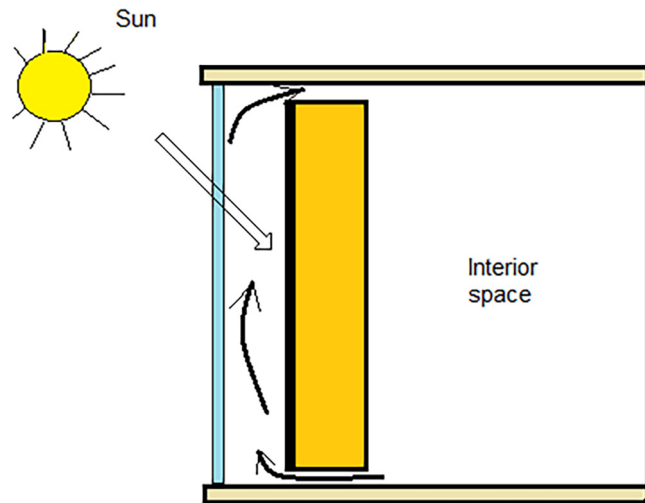


Fig. 1. Principles of Trombe wall.

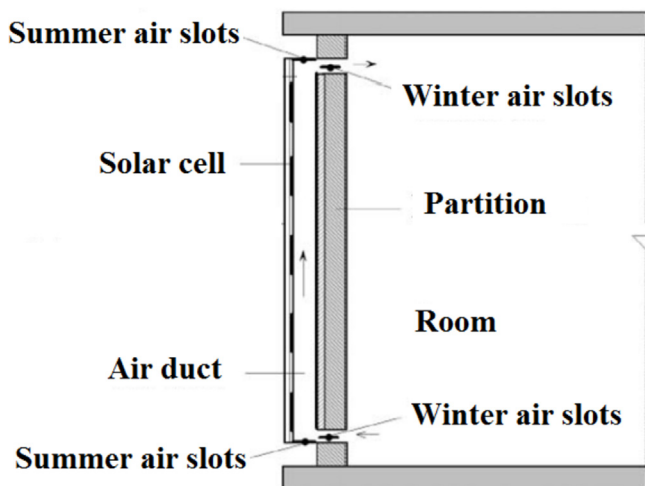


Fig. 2. Schematic of PV/TW system.

system with a normal Trombe wall-solar cell. However, For matching the voltage requirement of the system, the DC fan was connected to a separate PV module. It was showed that the assisted DC fan could be improved in some level the averaged temperatures of the room and PV cells. However, the trends of electrical performance is not well captured due to the lacking of measured data. Furthermore, the optimum fan speed and the fan's energy consumption did not involved. In some level Yi et al. [14] investigated the influence of DC fan on the performance of PV/TW system through a simulation model. It was noted that as the fan speed increases, the average room temperature and thermal efficiency improve firstly and then deteriorate, while there was un conspicuous augmentation in electrical efficiency. Even so, the impact of the energy consumption of DC fan on the overall efficiency of the system's was not considered. Ji et al. [15] studied the electrical and thermal performance of PV/TW utilized in Tibetan residential buildings based on simulation model. It was confirmed that when the width of PV/TW increased, the room temperature also increased, although electrical effectiveness was almost constant. Also, the wall insulation improved thermal performance significantly but reduced electrical performance slightly. However, it was

deduced the feasibility of the developed model based on the climate data generated by a software analysis. Moreover, there is no real verification about the reliability of the model result. Hu et al. [16] investigated experimentally three configurations of PV/TW module in China, these modules are PVBW, PVGTW and PVMTW. The study confirmed that the blind angle of PV and the entry air flow rate of 50° and 0.45 m/s, respectively, were the best parameters for the overall performance of PV/TW system. However, these findings were provisionally based on the working ambient conditions and the configuration of the PV/TW module. Sun et al. [17] concluded that the thermal efficiency of PV/TW system was affected by design parameters through numerical simulation. However, the correlation between the performance of the building design and the PV/TW system needs to be further clarified according to the ambient environments and latitude location. Yang et al. [18] offered a validated numerical investigation on thermal and electrical behavior of PV/TW system. The validity of the simulation model was confirmed with reasonable predictions based on the velocity distribution across the air duct measured by a LDA system. It was revealed that, an improved performance of the ventilated PV modules could be achieved with lower height and deeper depth of the air duct. A sound designed PV/TW system could be decreased the temperature of the solar cell by 15°C and increased the electrical power generation by 8% in comparison with the non-ventilated wall. It was recommended to minimize the air channel dimensions as low as possible to prevent choking of the ventilation flow rate. However, the overall system efficiency does not evaluated which deserves further investigation.

According to the above survey, among several techniques have been employed to improve the performance of PV/TW system there is no one previously used the porous medium. Moreover, it can be concluded that there are some argument about the influence of the DC fan, in terms of energy consumption and air velocity, and glass cover on the system performance. The aim of this paper is to carry out an experimental and theoretical investigations of the enhancement of thermal and electrical performance of the PV/TW system through inserting of a porous medium, a DC fan, and a glass cover.

2. Methodology

The exploitation of solar energy to generate electricity is one of the most famous applications in the developed countries, but the major disadvantage of solar cells is their high temperature, which leads to reduce their productivity, especially in the hot climate, as in Iraq. The improvement of the efficiency of the solar cells was achieved by withdrawing the generated heat and utilizing it for the domestic applications. It is well known that porous material is one of the important techniques for storing heat and use it in cloudy skies or at night. The present study aims to study the influence of the porous medium on the performance of the PV/TW system. The summary of this paper is as follows: details of the practical part are described in section 3, where the experimental work of the PV/PV/TW system is described. In section 4, the mathematical relations and performance estimation are offered and explained. The results are clarified and discussed in section 5; then the conclusions and recommendations are summarized in section 6.

3. Experimental work

This study was conducted at Kirkuk city, northern Iraq (Lat. 33.46°E , North and Long. 44.39°E East) from December 2017 to February 2018. Experimental data were recorded from 9 a.m. to 4 pm. Two symmetrical practical models of PV/TW system, as seen in Fig.(3), were built to study the influence of operational, design and

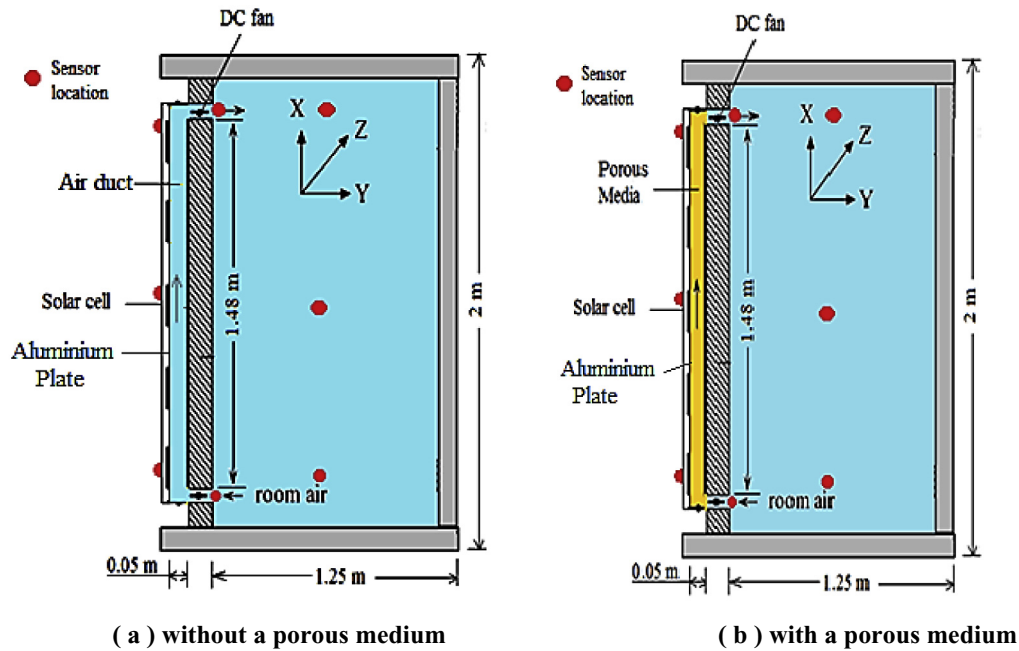


Fig. 3. Experimental set-up.

climatic conditions on the system performance. The first practical model, as shown in Fig. (3-a), consists of a glass panel, a solar cell, an aluminum plate a duct for airflow and the room wall. The test rooms were constructed from the sandwich panel and have been well insulated to reduce the thermal losses. The dimensions of the tested rooms were 2 m height, 1.25 m width and 1.25 depth, where the PV panel attached to the southern faces, as shown in Fig (4). The experimental set-ups were facing to the south to increase the solar energy incident on the Trombe wall. Other important details and dimensions are shown in Fig (3).

Solar cells of the Polycrystalline type operated as heat absorbing surface. Table (1) describes the specifications of the solar cell. To study the effect of the glass cover, it was fixed on the front surface

of the solar panel. The air duct in both models is composed of the following dimensions (height 2 m width 0.68 m and thickness 0.1 m). It contains two openings at the top and bottom to rotate the air. The sides of the air duct well insulated from the sides using glass wool with thermal conductivity of $0.035 \text{ W/m} \cdot ^\circ\text{C}$ [19]. The air duct of the second configuration (see Fig. 3-b) is the same as the air duct for the first configuration (see Fig. 3-a) except the air duct was filled with porous medium.

Porous medium consisted of glass pellets with 16 mm diameter and thermal conductivity of $0.78 \text{ W/m} \cdot \text{K}$ [20]. The porosity of the glass pellets was measured and it was equal to 0.437. Two DC fans for each PV/TW system are fixed at the exit of the air duct to draw the hot air from the inlet duct and pass it through the duct. The velocity of air through the duct was measured by using a multi-functional anemometer device.

The two fans working on a DC current were connected in parallel and they can operate even on cloudy days. Temperature measurement is considered one of the important factor for determining the performance of the PV/TW system. It is also considered the principle parameter to determine its efficiency. 10- thermometers were fixed at selected locations for each model to measure temperature. Six thermometers were mounted at the top, bottom, and center of each room and solar cell distributed along the cell which were separated by 50 cm between each thermometers. Two thermometers were also mounted at the inlet and outlet of air. Moreover, two thermometers were employed to measure the temperature of ambient and the glass surface. Solar meter (SM206) was utilized to measure solar radiation at the same level of the solar cell. A battery was used to store the electricity generated by the cells. Multi-meter was utilized to measure the voltage and current as shown in Fig. (5). The DC fans were connected to the battery which utilized to rotate the air to cool the solar cell.

4. Mathematical model formulation

In this part, a mathematical model is constructed for the PV/TW system, as shown in Fig.(6), which used to generate electricity and heating the air. It includes the computation of the temperatures of



Fig. 4. A photograph of the experimental test rooms.

Table 1
Specification of solar cell.

Parameters	Unit	Parameters	Unit
Maximum Power at the standard condition	150 W	Short Circuit Current (I_{sc})	8.81 A
Maximum Power voltage	17.9 V	Operating Temperature	25 °C
Maximum Power Current	8.38 A	Cell Type	Polycrystalline
Open Circuit Voltage (V_{oc})	22.4 V	Dimensions (mm)	1.48 × 0.68 × 0.035 m

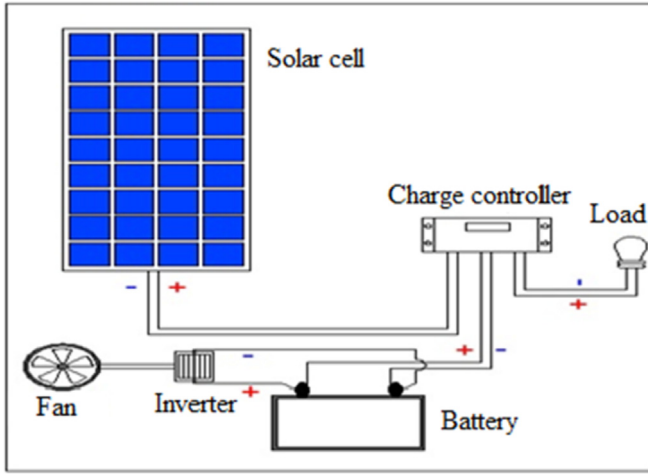


Fig. 5. Solar cell with accessories.

system were evaluated. Models that have been built for the PV/TW system with and without the DC fan and porous medium. An energy balance was performed after assuming the following hypotheses [21–23]:

1. The system operates under quasi-steady-state conditions.
2. There is no leakage from the air duct.
3. The flow is one dimensional i.e. the temperature of the flowing air varies only in the direction of flow (x-direction).
4. There is no temperature gradient across the thickness of the solar cell and wall.
5. Sky temperature is assumed to be equal to ambient air temperature.
6. Heat transfer by conduction across porous medium is negligible.
7. Neglecting the effect of heat transfer across the walls (North, East, and West).

Based on the hypotheses listed above, energy balance equations have been applied to the PV/TW system, which includes the solar cell, aluminum plate, and air duct.

4.1. Energy balance analysis of the solar cell

The solar cell not only generates electrical power, but also it gains thermal energy. So the following equation describes the energy balance of the solar cell [24,25]:

$$G \cdot \alpha_c = E + U_T(T_c - T_a) + U_{bottom}(T_c - T_p) \quad (1)$$

Re-arrange the eq. (1), the temperature of the solar cell was calculated as:

$$T_c = \frac{G \cdot \alpha_c - E + U_T T_a + U_{bottom} T_p}{U_T + U_{bottom}} \quad (2)$$

where E is the electrical power output of the solar cell and can be calculated according to the following expression [13]:

$$E = G \cdot \alpha_c \cdot \eta_{ele,s} \cdot (1 - 0.0045 \cdot (T_c - 298.15)) \quad (3)$$

where $\eta_{ele,s}$ is the efficiency of the solar cell at standard conditions (1000 W/m², 25 °C).

U_T : is the overall heat transfer coefficient between solar cell and ambient which is evaluated according to the following expression [26,27]:

$$U_T = \left[\frac{1}{h_{c,c-a}} + \frac{1}{h_{r,c-a}} \right]^{-1} \quad (4)$$

$h_{c,c-a}$, $h_{r,c-a}$ are the convective and radiant heat transfer coefficients on the outside surface of the solar cell and they are given according to the following expressions [10,28,30]:

$$h_{c,c-a} = 5.7 + 3.8 \times V \quad (5)$$

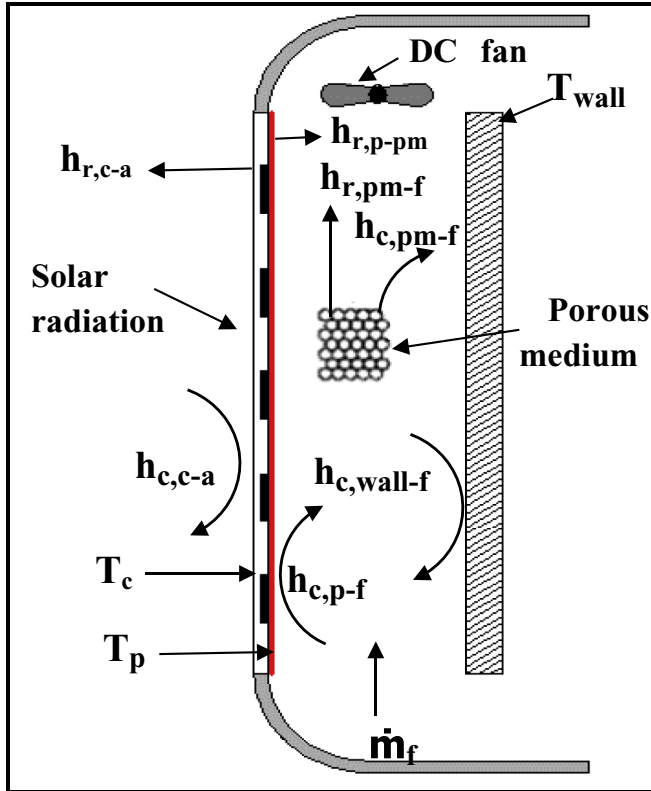


Fig. 6. Schematic and nomenclature of the PV/TW system.

the solar cell, the aluminum plate as well as the temperature gradient of the air along the duct. According to these computed temperatures, the electrical and thermal efficiencies of the PV/TW

$$h_{r,c-a} = \varepsilon_1 \cdot \sigma \cdot (T_c^2 + T_a^2) \cdot (T_c + T_a) \quad (6)$$

The emissivity factors ε_1 for the front of the solar cell can be calculated from [5,28,29]:

$$\frac{1}{\varepsilon_1} = \frac{1}{\varepsilon_c} + \frac{1}{\varepsilon_a} - 1 \quad (7)$$

where ε_c and ε_a are the emissivities of the solar cell and ambient, respectively.

U_{bottom} : is the overall heat transfer coefficient between the solar cell and aluminum plate which is evaluated according to the following expression [26,27]:

$$U_{bottom} = \left[\frac{L_{si}}{\lambda_{si}} + \frac{L_p}{\lambda_p} \right]^{-1} \quad (8)$$

where L_{si} , λ_{si} , L_p , and λ_p are the thickness of solar cell, thermal conductivity of solar cell, thickness of aluminum plate and thermal conductivity of aluminum plate, respectively.

4.2. Energy balance analysis of the aluminum plate

Energy balance for an aluminum plate of the model with porous medium can be represented by the following equation [21,23]:

$$\begin{aligned} U_{bottom} (T_c - T_p) + \tau_g \alpha_p (1 - \beta_c) G \\ = h_{c,p-f} (T_p - T_f) + h_{r,p-pm} (T_p - T_{pm}) \end{aligned} \quad (9)$$

In case of the empty duct, without porous medium, the (T_{pm}) in the last term replaced by (T_w) . Where, $h_{c,p-f}$ is the convective coefficient of heat transfer between the air flowing through the porous medium and the aluminum plate which is calculated as [21,23]:

$$h_{c,p-f} = \frac{Nu_{pm} \cdot \lambda_f}{\varphi \cdot D_{hd}} \quad (10)$$

D_{hd} the equivalent diameter of the porous medium, which is given as [21]:

$$D_{hd} = \frac{2\varphi d_{pm}}{3(1-\varphi)} \quad (11)$$

d_{pm} is the particle diameter and φ is the porosity of the porous medium which computed as:

$$\varphi = \frac{V_f}{V_t} \quad (12)$$

where $h_{r,p-pm}$ is radiation coefficient of heat transfer from aluminum plate to the porous medium ($W/m^2.K$), which is calculated based on the following expression [21]:

$$h_{r,p-pm} = \varepsilon_2 \cdot \sigma \cdot (T_p^2 + T_{pm}^2) \cdot (T_p + T_{pm}) \quad (13)$$

The temperature of the aluminum plate can be evaluated from:

$$T_p = \frac{U_{bottom} T_c + h_{c,p-f} T_f + h_{r,p-pm} T_{pm} + \tau_g \alpha_p (1 - \beta_c) G}{h_{c,p-f} + h_{r,p-pm} + U_{bottom}} \quad (14)$$

4.3. Energy balance analysis of the air flowing in the duct

Energy balance for air flowing in the duct with the porous medium can be represented by the following equation [21]:

$$\begin{aligned} \frac{C_{pf} \cdot \dot{m}_f}{w} \frac{dT_f}{dx} = h_{c,p-f} (T_p - T_f) + h_{c,wall-f} (T_{wall} - T_f) \\ + h_{c,pm-f} (T_{pm} - T_f) \end{aligned} \quad (15)$$

In case of the empty duct, without porous medium, the last term is omitted.

$$\text{where, } \dot{m}_f = \rho_f \cdot D \cdot W \cdot V_f \quad (16)$$

V_f is the air velocity in through the duct. For natural convection, it can be calculated as follows [13]:

$$V_f = \sqrt{\frac{0.5 \cdot g \cdot \bar{\beta} \cdot X \cdot (T_{f,out} - T_{f,in})}{C_f \frac{X}{d} + \frac{C_{in} \cdot A_{in}^2}{A_{in}^2} + \frac{C_{out} \cdot A_{out}^2}{A_{out}^2}}} \quad (17)$$

where $\bar{\beta}$ is the reciprocal of the mean air temperature; A_{out} and A_{in} are the areas of the top and bottom vents, respectively; C_{out} , C_{in} are the loss coefficients at the top and bottom vents, respectively; C_f is the friction factor along the air duct, the values of these factors are specified as follows [13]:

$$C_f = 0.3 \times 1.368 \times G_{rx}^{0.084} \quad (18)$$

$$C_{in} = 0.25, \quad C_{out} = 0.3$$

$$\bar{\beta} = \frac{1}{T_f} = \frac{2}{T_{f,in} + T_{f,out}} \quad (19)$$

For forced convection condition, the air velocity, V_f , is conveniently correlated to incident solar radiation (G), as follow [13,14]:

$$V_f = C_{fan} \cdot G \quad (20)$$

where C_{fan} is the correlation constant has a unit of m^3/J . To specify the value of C_{fan} , the measured data of the air velocity through the duct with assisted DC fan was plotted versus the incident solar radiation, as shown in Fig. 7. The slope of the best fitting line represents the value of C_{fan} . According to the measurement of current experimental work, the value of C_{fan} was equal to $(0.0006) m^3/J$.

The convective coefficient of heat transfer from the aluminum plate to the air flowing through the duct without porous medium,

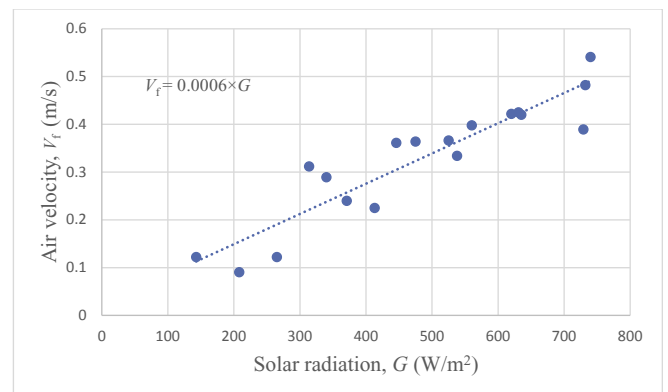


Fig. 7. The air velocity in the air duct versus the incident solar radiation.

$h_{c,p-f}$, is assumed to be equal to $h_{c,wall-f}$ [24,25]. For air following through duct filled with porous medium, it can compute the coefficient of heat transfer by convection ($h_{c,pm-f}$) using the following correlation [23]:

$$h_{c,pm-f} = \left[\frac{1}{h_{pmf}} + \frac{D_{hd}}{\beta_{pm} \lambda_{pm}} \right]^{-1} \quad (21)$$

β_{pm} is a constant depends on the porous medium shape. h_{pmf} can be evaluated as [21,23]:

$$h_{pmf} = \frac{Nu_{pm-f} \lambda_f}{D_{hd}} \quad (22)$$

$$Nu_{pm-f} = \left(\frac{0.255}{\phi} \right) Re_{pm}^{0.75} Pr_f^{1/3} \quad (23)$$

where Re_{pm} is Reynold's number for the porous medium duct which is calculated according to the following equation [21,23]:

$$Re_{pm} = D_{hd} \frac{\dot{m}_f}{A_m \mu_f} \quad (24)$$

where A_m is the specific wetted area; defined as, the heat transfer surface area of the porous medium wetted by the flowing air and evaluated according to the following equation [21,23]:

$$A_m = \frac{6(1-\phi)}{d_{pm}} \quad (25)$$

λ_{pm} is the effective thermal conductivity the porous medium duct which is calculated according to the following equation [21,23]:

$$\lambda_{pm} = \phi \lambda_f + (1-\phi) \lambda_g \quad (26)$$

4.4. Evaluation of thermal and electrical efficiencies

The thermal efficiency of the PV/TW system can be calculated as follows [25]:

$$\Delta_{th} = \frac{\dot{m}_f C_p (T_{f, out} - T_{f, in})}{G \cdot A_c} \quad (27)$$

Also, the electrical efficiency of the PV/TW system is calculated by the following equation [5]:

$$\eta_{ele} = \frac{V_o \cdot I}{G \cdot A_c} \quad (28)$$

The overall system performance can be assessed based on the total efficiency of the hybrid PV/TW system which is summing both thermal and electrical efficiencies.

A computer program was built in MATLAB software to solve the mathematical equations that mentioned above. The characteristics and dimensions of the model presented and the solar cell that utilized in this article are clarified in Table (2).

5. Results and discussions

In this section, the typical results obtained from the tests were presented. The tests started from 9 a.m. until 4 pm. The results were compared experimentally with and without a porous medium under different climate conditions in Kirkuk city at the north of

Iraq. This article dealt with the following five case studies:

- 1- PV/TW system without DC fans and without porous medium (the base case).
- 2- PV/TW system using DC fans to circulate the air without porous medium.
- 3- PV/TW system using porous medium without DC fans.
- 4- PV/TW system using porous medium with DC fans to circulate the air.
- 5- PV/TW system using porous medium with DC fans to circulate the air and glass cover.

5.1. Results of the system without a porous medium

Fig. 8 shows the hourly variation of solar cell temperature for the PV/TW system with and without DC fans. It can be seen that there is a reduction in the cell temperature as the DC fan inserted. Without using the fan, the solar cell temperature ranged between 26 °C and 58 °C with ultimate value at 12 noon. After this time the temperature of the solar cell was reduced, this is due to the net solar radiation absorbed becomes lower. While with using DC fan, the solar cell temperature ranged between 25 °C and 45 °C with ultimate value at 11 am. These reductions in the temperature of the cell are increasing its conversion efficiency. This agrees with the results of the performance of the most PV/TW system [13,17]. Even though, it can be noted that there are some fluctuations in the results which are attributed to the change of weather conditions as well as the uncertainties of measurement instruments. The same behavior was appeared for the variation of the outlet temperature of the air duct as shown in Fig. (9). It's noted that the temperature of exit air from the duct was varied with time and reached the maximum value at 12 noon. Moreover, it can be seen that after 15 p.m. the temperature of exit air from duct without DC fan is greater than its value in the case with DC fan. This is attributed to the absence of the sun and the ambient temperature was higher in case with DC fan. This is resulting in a low DC fan speed and therefore the electric power is greatly reduced (see Fig. 12).

Fig. 10 clarifies the influence of using the DC fan on the room temperature, where the fan increases the rate of heat transfer from the solar cell to the air which goes to the room. The maximum value was 25 °C for the particular day, which occurred at 1 p.m., and then it decreased in the late afternoon. Fig. 10 reveals a slight difference in ultimate room temperature occurred during a typical day when using a fan to circulate the air. The experimental results collected from this study showed a significant effect of using the fan on the mean room temperature. These results were consistent with the results of the other researchers [12–14]. Also, it is noted there are some fluctuation in the results which is attributed to the change of weather conditions as well as the uncertainties of measurement instruments. Fig. (11) indicates a good correlation between practical results and the mathematical model results. The difference between the theoretical and the practical results is less than 4% for the solar cell temperature, which is considered a good result. Also, it is noted that the theoretical values of the temperature of the solar cell are higher than the experimental values due to excluding the effect of the convection heat losses from the sides.

Fig. 12 illustrates the daily pattern of solar radiation and the produced electrical power of a typical day. For the base case (without DC fan), three lamps (with 24 V per lamp) were used as a load, while in case of using DC fan the three lamps and two DC fans were considered as a load. It can be deduced that the produced electrical power follows the trends of solar radiation. It is clearly revealed the enhancement in electricity production as the DC fan inserted. This is due to reducing the PV cell temperature as a result of rotating air behind the cell which is carrying extra heat gain.

Table 2

The characteristics and dimensions of the system.

Glass cover	Solar cell	General properties of the system
Glass thickness $\delta_g = 4$ mm $\rho_g = 2200$ kg/m ³ $c_g = 480 \frac{J}{kg \cdot K}$ Thermal conductivity $k_g = 1.1$ W/(m. K) $\alpha_g = 0.05$, $\beta_c = 0.83$ $\epsilon_g = 0.9$, $\tau_g = 0.9$	η_{el} at normal condition (25 °C) = 15.5% Thickness of solar cell (δ_{sc}) = 3 mm Solar cell density (ρ_{PV}) = 2330 kg/m ³ Thermal conductivity $k_c = 87$ W/(m. K) Absorptivity of the solar cell $\alpha_{PV} = 0.94$ Emissivity of solar cell $\epsilon_c = 0.88$	Aluminum thickness $\delta_{al} = 1$ mm Dimensions of the plate (106 × 52) cm Thickness of insulation (L_b) = 3.5 cm The thermal conductivity of the insulation $k_b = 0.035$ W/(m. K) The distance between the glass cover and solar cell = 10 cm Thermal conductivity of Aluminum $k_{al} = 204$ W/(m.K)

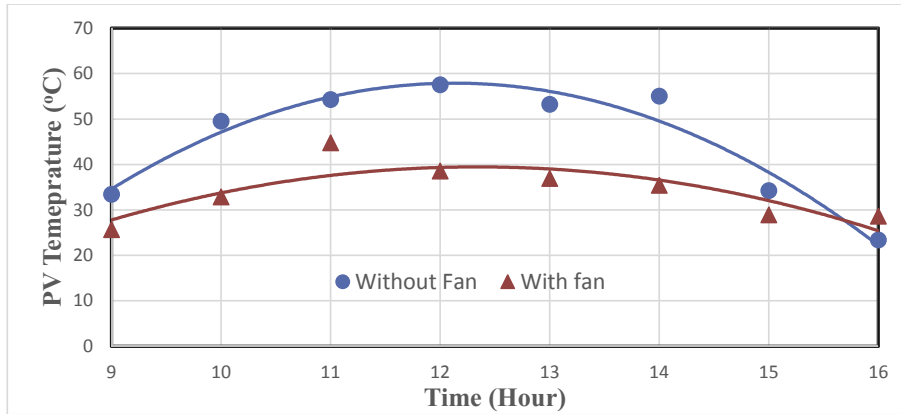


Fig. 8. Effect of DC fan on hourly variation of PV cell temperature (10 and 25/12/2017).

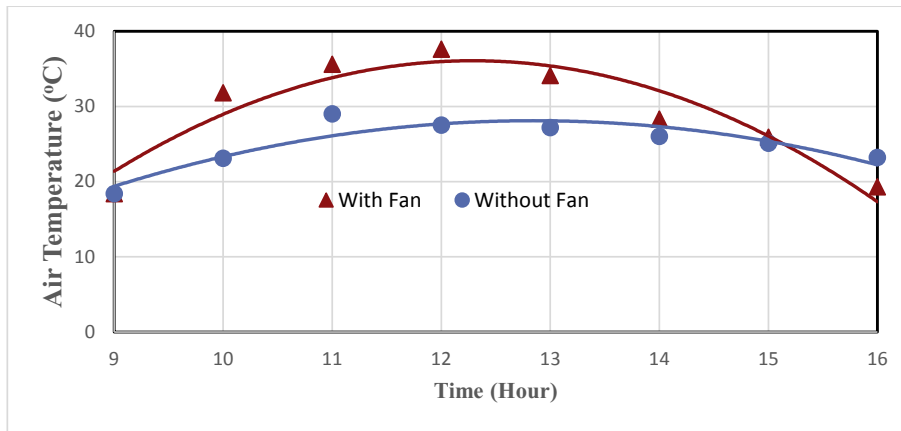


Fig. 9. Effect of DC fan on hourly variation of air exit temperature (10 and 25/12/2017).

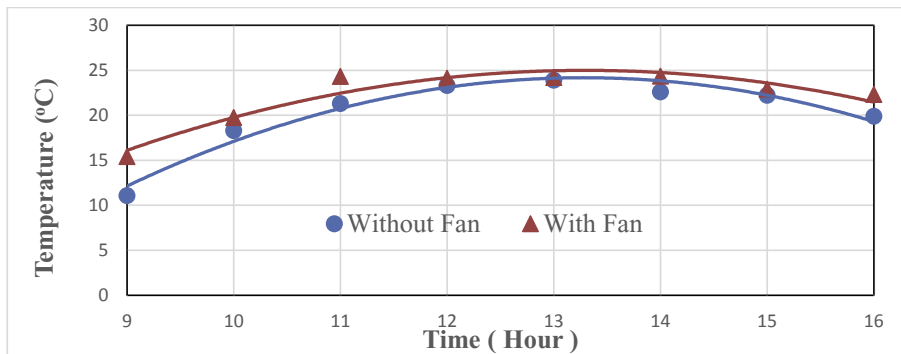


Fig. 10. Effect of DC fan on hourly variation of the room temperature (10 and 25/12/2017).

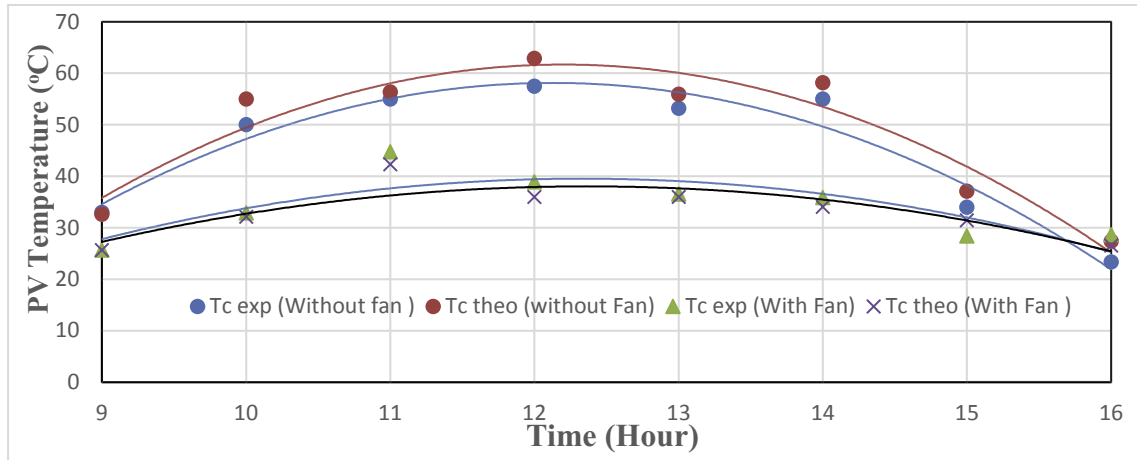


Fig. 11. Comparison between the practical and theoretical results of solar cell temperature.

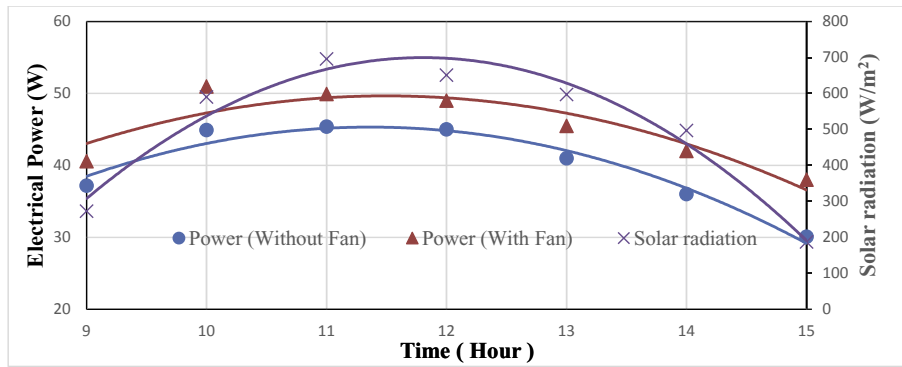


Fig. 12. Influence of DC fan on hourly variation of the produced electrical power (10 and 25/12/2017).

5.2. The performance of PV/TW system with porous medium

The porous medium is utilized in many fields of applied engineering. It is widely used to boost the rate of heat transfer due to the increased surface area of heat transfer as well as its ability to store heat [32]. A number of tests were performed to show the effect of the porous medium on the performance of the PV/TW system without using the fan. Fig. 13 clarifies the effect of porous medium on the solar cell temperature without DC fan. It is indicated that the solar cell temperature of PV/TW system without porous medium is higher as compared to its values for the system with porous medium until 2 p.m. This is because of the most

absorbed solar energy has been used to heat the porous medium (glass spheres). After 2 p.m. the solar cell begins to gain heat from the porous medium. This behavior is typical for a porous Trombe wall as reported by previous studies [2,3]. Good consistence was achieved between theoretical and practical results of this case as shown in Fig. (14). Again, it is noted there are some fluctuation in the results which is attributed to the change of weather conditions as well as the uncertainties of measurement instruments.

The behavior of mean room temperature through a typical day with and without porous medium is clarified in Fig. 15. It was observed that the mean air temperature inside the experimental room increased with time up to 1 p.m. and then decreased. This is

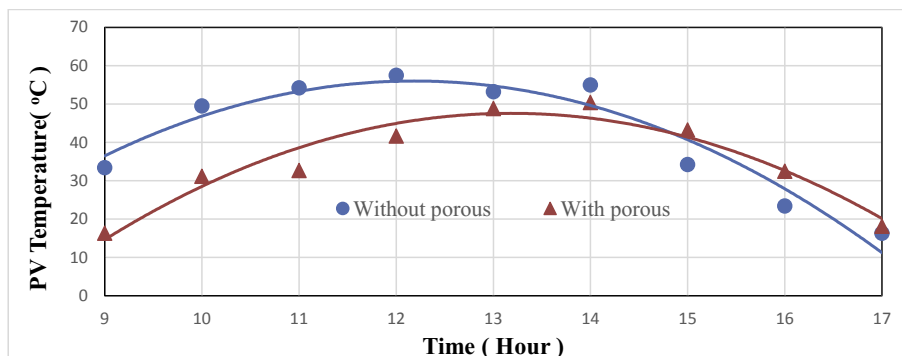


Fig. 13. Effect of porous medium (without fan) on hourly variation of PV cell temperature (14 and/1/2018).

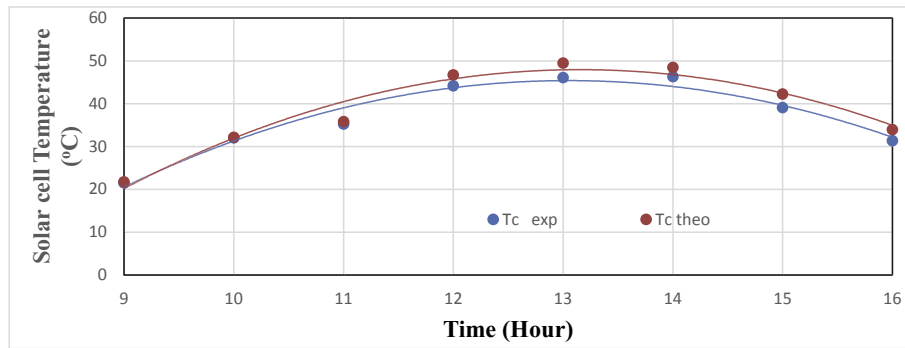


Fig. 14. Theoretical and practical results of hourly variation of solar cell temperature (with porous medium and without DC fan).

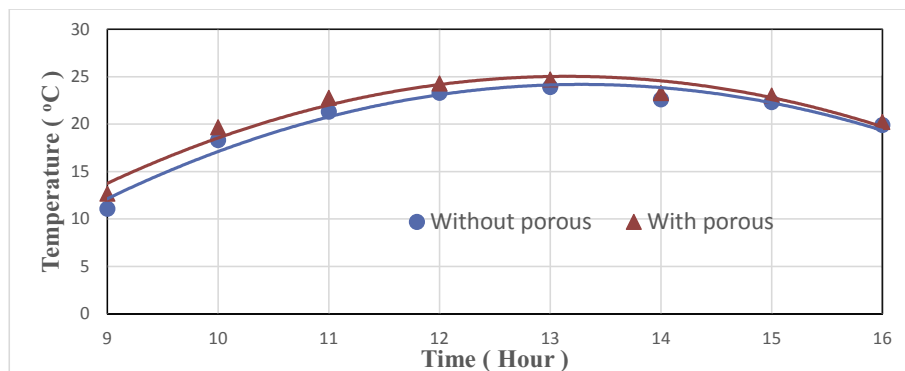


Fig. 15. Effect of porous medium on hourly variation of the room temperature (without fan) (14 and 15/1/2018).

because the heat losses become just larger than the heat energy comes from PV/TW system. This is in line with previously published results of most studies [33]. It is also noted that the use of the porous medium in the PV/TW system leads to a slight increase in room temperature which is economically feasible.

Fig. (16) shows the effect of porous medium on the produced electrical power. The presence of the glass pellets leads to increase the electrical power which produced from the solar panel. This is explained by the fact that the porous medium works to absorb the heat from the solar cell which cools it and thus increase the electrical power production [2]. Again, it is noted there are some fluctuation in the results which is attributed to the change of weather conditions as well as the uncertainties of measurement instruments.

Table 3 shows the hourly percentage of an increase in the mean room temperature and a decrease in the solar cell temperature compared to the reference case (without DC fan and without porous medium). Generally, it can be indicated that there is always

an increase in mean room temperature and a reduction in solar cell temperature as the DC fan and porous medium are involved. However, there is no clear trend for the rate of increment or reduction could be elaborated because of the system was exposed to various climatic conditions.

5.3. Influence of glass cover on the performance of PV/TW

This section will analyze the performance of the glazed and unglazed PV/TW system (with porous medium and fan to circulate the air). The glass cover on the PV/TW system was used to minimize the heat losses to the surrounding. This changes in solar radiation made a “greenhouse phenomena” and increased the thermal energy stored inside the system [10,34]. Although, the transparent glass cover also increased the reflection of thermal radiation on the glass cover and then caused a decrease in the benefits of energy. To study the effect of the glass cover, a number of tests were conducted to understand this effect. It was obvious that the glazed configuration had a higher value of the solar cell and mean room temperatures than the unglazed design as shown in Figs. (17 and 18). It is clear from this figures that the temperature of the solar panel was 67 °C at 1 p.m. Fig. (18) shows that the mean room temperature for the glazed system is higher than the mean air temperature in the unglazed system, and this was due to the higher thermal losses from the front face of the system for the unglazed system.

Fig. (19) shows the variation of the produced electrical power during the day. It is seen that the produced electrical power of the glazed system is lower than the unglazed one. This is due to an increase in the solar cell temperature in the glazed system which causes a reduction in the produced electrical power. The higher thermal gain of the glazed PV/TW system is very important for the

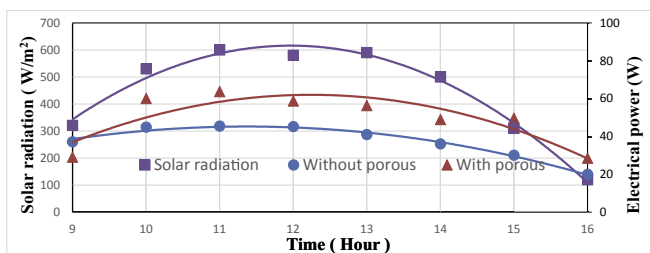


Fig. 16. Effect of porous medium on the produced electrical power (without fan) (14 and 15/1/2018).

Table 3
Percentage of increase in room temperature and decrease in the solar cell temperature.

Time	$\Delta T_c\%$ with DC fan	$\Delta T_c\%$ with porous	$\Delta T_c\%$ with DC fan and porous	$\Delta Tr\%$ with DC fan	$\Delta Tr\%$ with porous	$\Delta Tr\%$ with DC fan and porous
9	23.3	21.3	16.1	39.2	59.7	26.8
10	33.7	33.1	2.5	7.8	12.9	15.5
11	10.2	32.5	27.7	14.1	11.6	9.7
12	6.9	18.9	17.5	8.1	13.3	14
13	4.3	8.2	23.2	10	16.6	12.8
14	17.5	8.4	2.1	12.1	16.2	8.7
15	15.7	38	45.8	3	3.5	9.2
16	16.8	35.6	41.7	12.1	1.7	3.9

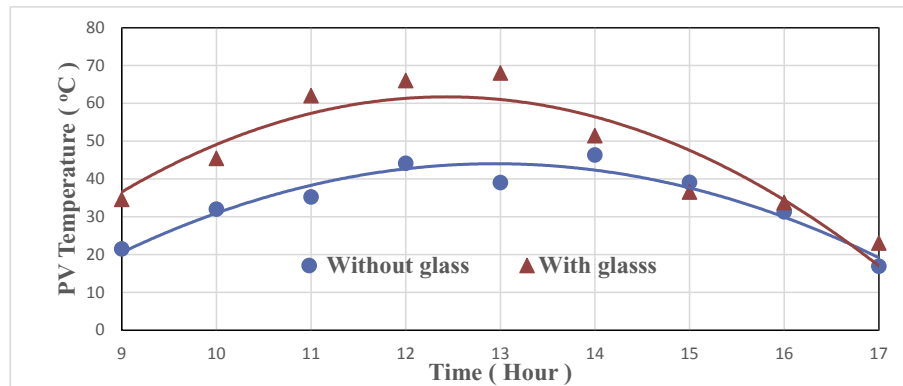


Fig. 17. Effect of glass cover on hourly variation of solar cell temperature (21 and 28/1/2018).

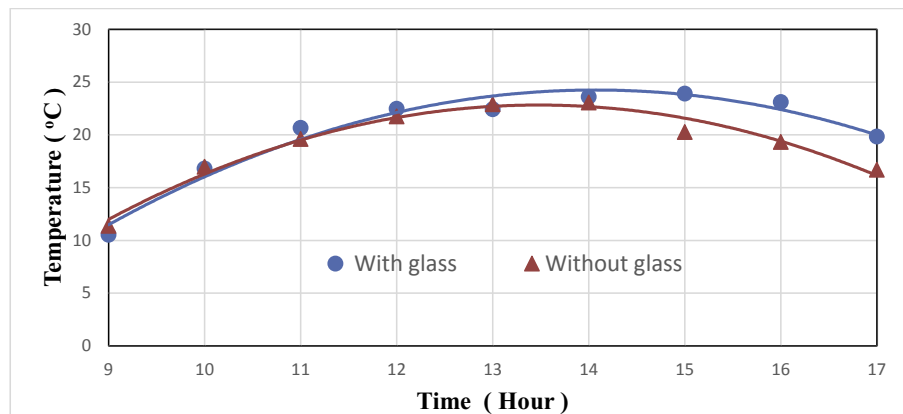


Fig. 18. Effect of the glass cover on hourly variation of the room temperature (21 and 28/1/2018).

substantial applications of air heating. On the other hand, the produced electrical power for the unglazed system was higher than the glazed system.

Presence the glass panel in the front of the PV/TW system caused an increase in the solar cell temperature and led to more reduction in the electrical power. Accordingly, the use of the glass panel in the PV/TW system is an undesirable option for electrical generation only. Generally, the glazed model has a higher compound power output (thermal and electrical) than the unglazed PV/TW system. These results were consistent with the results of previously published works [10,16].

5.4. Efficiency of PV/Trombe wall system

Table (4) illustrates the values of the thermal and electrical efficiencies for different system configurations. These results show that the presence of the DC fan increases the values of thermal and

electrical efficiency by 5.48% and 3.04%, respectively. It can be seen that the presence of the porous medium increases the values of thermal and electrical efficiency by 9.07% and 3.60%, respectively. While, for the PV/TW system with DC fan and porous medium the increment of values of thermal and electrical efficiencies were about 12.83% and 3.93%, respectively. Also, it is seen that the thermal efficiency of the glazed PV/TW system is higher than the unglazed one (the increment about 19.9%). This trend was due to the increase in the thermal losses in the unglazed system. The higher value of thermal efficiency of the glazed PV/TW system is very important for the main utilization of air heating. On the other hand, the electrical efficiency of the glazed system was just little bit higher than the unglazed one (the increment about 0.5%). But should be in mind, the presence of glass cover leads to diminish the enhancement of electrical performance, which is achieved by the DC fan and porous medium. Setting a glass layer in the front of the system caused an increase in the solar cell temperature and led to

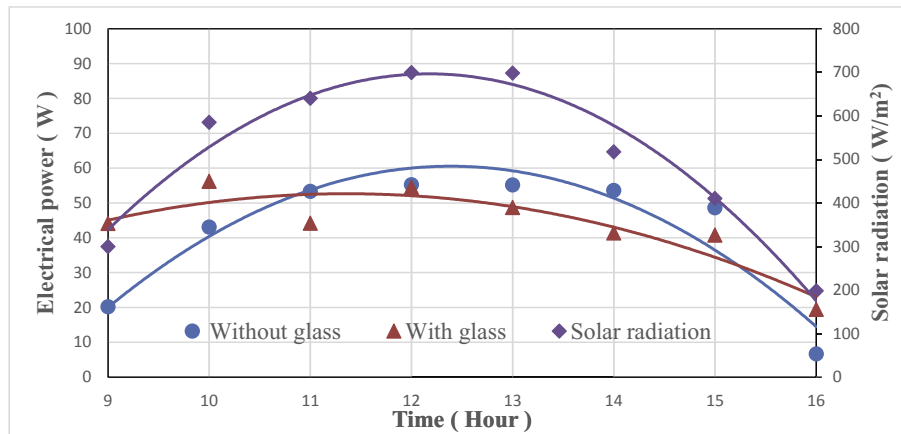


Fig. 19. Effect of the glass cover on hourly variation of the produced electrical power (21 and 28/1/2018).

Table 4

The hourly and daily average system efficiencies for various configuration.

	9 a.m.	10 a.m.	11 a.m.	12 a.m.	1 p.m.	2 p.m.	3 p.m.	4 p.m.	Daily Efficiency (%)
η_{th} without Fan	20.4	40.88	41.87	40.85	33.36	25.41	20.6	16.7	30
η_{ele} without Fan	8.27	6.66	5.71	6.057	6.68	7.86	5.18	3.2	6.28
η_{th} with Fan	23.2	42.54	47.59	48.59	39.82	31.92	27.78	22.41	35.48
η_{ele} with Fan	12.97	10.85	9.71	8.51	12.10	8.79	7.20	4.49	9.32
η_{th} with porous (without fan)	24.90	45.77	49.42	51.19	43.43	36.55	33.11	28.20	39.07
η_{ele} with porous (without fan)	13.7	11.91	10.90	8.86	10.35	9.55	9.0	4.77	9.88
η_{th} with (Fan + porous)	26.3	47.59	52.23	55.05	47.68	42.46	37.46	33.92	42.83
η_{ele} with (Fan + porous)	12.49	12.10	10.22	9.23	13.04	9.12	10.20	5.30	10.21
η_{th} With (Fan + porous + glass)	29.86	55.0	60.04	62.31	63.22	47.93	44.70	36.59	49.9
η_{ele} with (Fan + porous + glass)	6.65	8.19	8.84	10.24	7.30	5.56	4.33	3.19	6.776

more reduction in the electrical power. Accordingly, the presence of the glass cover in the hybrid PV/TW system is an undesirable choice for electrical generation only. An assessment of the overall system performance between all cases reveals that the porous medium has a compromise between the DC fan and glass cover effect. It is boosted both the thermal and electrical performance of the system without consuming or losing of system gain.

6. Conclusions and recommendations

From the results presented in the previous section, the following main conclusions and recommendations can be obtained:

1-Incorporating the PV/TW system with a DC fan improves its performance through a reduction in solar cell temperature and augmentation of heat gain, which enhance the overall system efficiency and room comfort condition.

2-Inserting the porous medium inside the air duct of the PV/TW system increases the area of heat transfer, which enhances its thermal and electrical efficiencies as well as improves the room comfort conditions.

3-The use of glass cover increases the temperature of the solar cell, which decreases the power and efficiency of the electricity generation. While increasing the room temperature and thermal efficiency.

4- The difference between the theoretical and the experimental results is less than 4% for the solar cell temperature, which is considered a good result. Also, it is noted that the theoretical values of the temperature of the solar cell are higher than the experimental values.

5-In terms of future investigations, it is suggesting to replace the porous medium by PCM material and inserting a cooling coil for

further system improvement.

References

- [1] Ahmed OK. A numerical and experimental investigation for a triangular storage collector. *Sol Energy* 2018;171(June):884–92.
- [2] Khalil Ahmed O, Aziz Mohammed Z. Influence of porous media on the performance of hybrid PV/Thermal collector. *Renew Energy* 2017;112:378–87.
- [3] Hu Z, He W, Ji J, Zhang S. A review on the application of Trombe wall system in buildings. *Renew Sustain Energy Rev* 2016;0–1. no. August 2015.
- [4] Ahmed OK, Hussein AS. New design of solar chimney (case study). *Case Stud Therm Eng* 2018;11(December 2017):105–12.
- [5] Jie J, Hua Y, Wei H, Gang P, Jianping L, Bin J. Modeling of a novel Trombe wall with PV cells. *Build Environ* 2007;42(3):1544–52.
- [6] Ahmed OK, Mohammed ZA. Dust effect on the performance of the hybrid PV/Thermal collector. *Therm Sci Eng Prog Feb.* 2017;3:114–22.
- [7] Xu XW, Su YX. Numerical simulation of air flow in BiPV-Trombe wall. *Adv Mater Res* 2013;860–863:141–5.
- [8] Irshad K, Habib K, Thirumalaiswamy N. Performance evaluation of PV-Trombe wall for sustainable building development. *Procedia CIRP* 2015;26:624–9.
- [9] Irshad K, Habib K, Thirumalaiswamy N. Implementation of Photo Voltaic Trombe Wall system for developing non-air conditioned buildings. In: *Proc - 2013 IEEE conf sustain util dev eng technol IEEE CSUDET 2013*; 2013. p. 68–73.
- [10] Irshad K, Habib K, Thirumalaiswamy N, Elmahdi AEA. Performance analysis of photo voltaic Trombe wall for tropical climate. *Appl Mech Mater* 2014;465–466(1):211–5.
- [11] Kundakci Koyunbaba B, Yilmaz Z. The comparison of Trombe wall systems with single glass, double glass and PV panels. *Renew Energy* 2012;45:111–8.
- [12] Kundakci Koyunbaba B, Yilmaz Z. The performance comparison of fan-assisted Trombe wall system. *A/J ITU J Fac Archit* 2013;10(2):198–211.
- [13] Jie J, Hua Y, Gang P, Bin J, Wei H. Study of PV-Trombe wall assisted with DC fan. *Build Environ* 2007;42(10):3529–39.
- [14] Yi H, Jie J, Hanfeng H, Aiguo J, Chongwei H, Chenglong L. Optimized simulation for PV-TW system using DC fan. In: *Proc ISES world congr 2007 sol energy hum settlement, sept 18–21, 2007*; 2008. p. 1617–22.
- [15] Ji J, Yi H, Pei G, He HF, Han CW, Luo CL. Numerical study of the use of photovoltaic - Trombe wall in residential buildings in Tibet. *Proc Inst Mech Eng Part a-Journal Power Energy* 2007;221(A8):1131–40.
- [16] Hu Z, He W, Hu D, Lv S, Wang L, Ji J, Chen H, Ma J. Design, construction and

- performance testing of a PV blind-integrated Trombe wall module. *Appl Energy* 2017;203(September):643–56.
- [17] Sun W, Ji J, Luo C, He W. Performance of PV-Trombe wall in winter correlated with south façade design. *Appl Energy* 2011;88(1):224–31.
- [18] Yang HX, Marshall RH, Brinkworth BJ. Validated simulation for thermal regulation of photovoltaic wall structures. In: *Conf Rec Twenty Fifth IEEE Photovolt Spec Conf - 1996*, vol. 3; 1996. p. 1453–6.
- [19] Duffie JA, Beckman WA. *Solar engineering of thermal processes*. fourth ed. John Wiley & Sons, Inc.; 2013.
- [20] Incropera FP, DeWitt DP, Bergman TL, Lavine AS. *Fundamentals of heat and mass transfer*. 2007.
- [21] Dhiman P, Thakur NS, Kumar A, Singh S. An analytical model to predict the thermal performance of a novel parallel flow packed bed solar air heater. *Appl Energy* 2011;88(6):2157–67.
- [22] Yousef BAA, Adam NM. Performance analysis for flat plate collector with and without porous media. *J Energy South Africa* 2008;19(4):33.
- [23] Ramadan MRI, El-Sebaai AA, Aboul-Enein S, El-Bialy E. Thermal performance of a packed bed double-pass solar air heater. *Energy* 2007;32(8):1524–35.
- [24] Mohd Nazari Abu Bakar HJ, Othman Mahmod, Din Mahadzir Hj, Manaf Norain A. Development of an improved photovoltaic/thermal (PV/T) solar collector with bifluid configuration. *Int J Chem Environ Eng* 2013;4(4).
- [25] Abu Bakar MN, Othman M, Hj Din M, Manaf NA, Jarimi H. Design concept and mathematical model of a bi-fluid photovoltaic/thermal (PV/T) solar collector. *Renew Energy* 2014;67:153–64.
- [26] AHMED OK, BAWA SM. The combined effect of nanofluid and reflective mirrors on the performance of PV/thermal solar collector. *Therm Sci* 2018; 1–16.
- [27] Sarhaddi F, Farahat S, Ajam H, Behzadmehr A, Mahdavi Adeli M. An improved thermal and electrical model for a solar photovoltaic thermal (PV/T) air collector. *Appl Energy* 2010;87(7):2328–39.
- [28] Peng J, Lu L, Yang H, Han J. Investigation on the annual thermal performance of a photovoltaic wall mounted on a multi-layer façade. *Appl Energy* 2013;112:646–56.
- [29] Rounis ED, Bigaila E, Luk P, Athienitis A, Stathopoulos T. Multiple-inlet BIPV/T modeling: wind effects and fan induced suction. *Energy Procedia* 2015;78: 1950–5.
- [30] Jie J, Wei H, Lam HN. The annual analysis of the power output and heat gain of a PV-wall with different integration mode in Hong Kong. *Fuel Energy Abstr* 2003;44(2):107. Jie, J. et al. *Solar Energy Materials and Solar Cells*, 2002, **71** (4), 435–448.
- [32] Craig S, Grinham J. Breathing walls: the design of porous materials for heat exchange and decentralized ventilation. *Energy Build* 2017;149:246–59.
- [33] Mohammed F, Khalil O, Emad A. Effect of climate and design parameters on the temperature distribution of a room. *J Build Eng* 2018;17(February): 115–24.
- [34] Iceri DM. Comparative analysis for glazed and unglazed collector for used in solar domestic hot watersystems. 2013. p. 2941–51. no. Cobem.